

# Dynamical fragmentation of flux tubes in the Friedberg-Lee model\*

S. Loh<sup>†</sup>, C. Greiner, U. Mosel and M.H. Thoma<sup>‡</sup>

Institut für Theoretische Physik, Universität Giessen

D-35392 Giessen, Germany

June 25, 2021

## Abstract

We present two novel dynamical features of flux tubes in the Friedberg-Lee model. First the fusion of two (anti-)parallel flux tubes, where we extract a string-string interaction potential which has a qualitative similarity to the nucleon-nucleon potential in the Friedberg-Lee model obtained by Koepf et al. Furthermore we show the dynamical breakup of flux tubes via  $q\bar{q}$ -particle production and the disintegration into mesons. We find, as a shortcoming of the present realization of the model, that the full dynamical transport approach presented in a previous publication fails to provide the disintegration mechanism in the semiclassical limit. Therefore, in addition, we present here a molecular dynamical approach for the motion of the quarks and show, as a first application, the space-time development of the quarks and their mean-fields for Lund-type string fragmentation processes.

---

\*Work supported by BMBF and GSI Darmstadt.

<sup>†</sup>Part of dissertation of Stefan Loh

<sup>‡</sup>Heisenberg Fellow

# 1 Introduction

During the collision of heavy nuclei at ultra-relativistic energies it is believed that the energy density reached may be high enough for a quark-gluon plasma (QGP) to be formed. Originally such collisions were assumed to be highly transparent [1, 2] and the two nuclei pass through each other keeping about half of their energies, though this might happen only at very high energies. On the other hand some of the individual target and projectile nucleons obtain a net color charge due to the exchange of gluons in the reaction zone. As a consequence, color flux tubes connecting these color charges, are built up as the nuclei recede. If the ions have sufficient energy, a large number of flux tubes may be produced, that may coalesce to a giant color flux tube or simply to an ensemble of individual flux tubes and color ropes (highly charged flux tubes) [3, 4, 5].

As kinetic energy of the ions is transferred to the color field between them it is believed that quark-antiquark and gluon pairs are created from the field via the Schwinger mechanism. If the pair creation rate is high enough, the parton density produced may be sufficient for a QGP to be formed. As the QGP expands and cools, hadronization begins. After hadronization is complete the hadron gas expands until the strong interactions freeze out and free hadrons are observed.

The present status of model descriptions of this scenario is the following: On the one hand there are the string- and parton-cascade-models (Fritjof [6], Venus [7], RQMD [8], HIJING [9], parton cascade [10]), that are based on phenomenological arguments and (or) perturbative QCD. However, all the nonperturbative mechanisms like string formation and decay and the final hadronization, are handled purely phenomenologically, i. e. by fragmentation prescriptions for the string breaking from fitting  $e^+e^-$ -data or by coalescence models [11, 12]. In order to gain more insight into the latter mechanism, effective models of QCD can be used, like the MIT-Bag model [13], the NJL-model [14, 15] or the various color dielectric models [16, 17, 18, 19]. Within these models there are attempts to describe the production of quark-antiquark

pairs in flux tubes [20, 21] or the collapse of flux tubes [22]. The main topics attacked in these works are the influence of the finite transverse size of the flux tube on the Schwinger pair production rate, or neutralization times for the strings via pair production, but not the full disintegration of flux tubes into physical mesons, which is needed in a consistent transport description of heavy ion collisions.

In this paper we consider flux tubes constructed in the Friedberg-Lee model, which has had many successes in other applications [16] and is a fully dynamical field theory with confinement. The quark degrees of freedom are handled via a transport equation derived by Elze and Heinz [23] (see also Blttel et al. [24]). In previous publications [25, 26, 27] we have investigated the dynamical confinement properties in nucleon-nucleon collision in the colorless version of the model as well as color-excitations in the full model, whereas here the outline is as follows:

In section 2 we give a brief introduction to the Friedberg-Lee model, and show how the parameters of the model can be fixed by static properties of hadrons and flux tubes. In section 3 we extract a string-string interaction potential by a dynamical fusion of two (anti-)parallel strings and in section 4 we present the full transport dynamical approach to the disintegration of a flux tube into mesons via quark antiquark particle production. After the discussion of some intrinsic problems connected with the semiclassical limit of the model, we give the space-time description of a string-fragmentation process of the Lund-type within a molecular dynamical approach.

## 2 The Friedberg-Lee model

The nontopological soliton model of Friedberg and Lee [17, 29], further developed by Goldflam and Wilets [30, 31], has enjoyed considerable interest in recent years, because it provides a dynamical description of hadrons as solitons of a selfinteracting mean field. Static solutions of this model have been studied extensively during the last decade [16, 31, 32], leading to a satisfactory description of hadronic properties.

In its original version the Lagrangian is given by

$$\mathcal{L} = \mathcal{L}_q + \mathcal{L}_{q\sigma} + \mathcal{L}_\sigma + \mathcal{L}_G , \quad (1)$$

where the various terms are as follows:

$$\mathcal{L}_q = \bar{\Psi}(i\gamma_\mu D^\mu - m_0)\Psi \quad (2)$$

describes the quarks as Dirac particles of current mass  $m_0 \approx 10 \text{ MeV}$ . The fermion wave functions have 4 (Dirac) times 3 (color) times  $n$  (flavor) components and the covariant derivative is  $D^\mu = \partial^\mu - ig_v(\frac{\lambda_a^\mu}{2})A_a^\mu$ , where  $A_a^\mu$  are the gluon fields that are coupled to the quarks covariantly. The term

$$\mathcal{L}_{q\sigma} = \bar{\Psi}g_0\sigma\Psi \quad (3)$$

describes the coupling of the quarks to the  $\sigma$ -field, which is assumed to mimic the long range and nonabelian effects of multi gluon exchange. The kinetic and potential part for the  $\sigma$  field

$$\mathcal{L}_\sigma = \frac{1}{2}(\partial_\mu\sigma)^2 - U(\sigma) \quad (4)$$

contains the self interaction potential  $U(\sigma)$  that is supposed to be quartic in the field,

$$U(\sigma) = \frac{a}{2!}\sigma^2 + \frac{b}{3!}\sigma^3 + \frac{c}{4!}\sigma^4 + B . \quad (5)$$

The constants in (5) are adjusted in such a way that  $U(\sigma)$  has a minimum at  $\sigma = 0$  and another, energetically lower one, at the nonzero vacuum expectation value  $\sigma_{vac}$ , where the potential is assumed to vanish. The constant  $B$  is chosen such that  $U(\sigma_{vac}) = 0$ . Since also  $U(0) = B$ ,  $B$  can be identified with the MIT-Bag constant, or the volume energy density of the cavity.

Color gluon fields are introduced as in QCD except for an interaction with the soliton field through a dielectric function  $\kappa(\sigma)$ ,

$$\mathcal{L}_G = -\frac{1}{4}\kappa(\sigma)F_{\mu\nu}^a F_a^{\mu\nu} , \quad (6)$$

with  $\kappa(0) = 1$  and  $\kappa(\sigma_{vac}) = 0$ .  $\kappa(\sigma)$  is not uniquely defined in this model, and a choice must be made as to its functional form. Several suggestions have been made in the past, that may be summarized to the general form

$$\kappa_{nm}(\sigma) = \left| 1 - \left( \frac{\sigma}{\sigma_{vac}} \right)^n \right|^m \Theta(\sigma_{vac} - \sigma) . \quad (7)$$

Friedberg and Lee [17] originally proposed  $n = m = 1$ , while others [33, 34] have suggested  $n = 1, m = 2$  or even  $(n, m) = (2, 1), (2, 3/2)$  and  $(2, 2)$  [35]. We prefer the parameters  $(n, m) = (1, 2)$ , for this choice guarantees a vanishing derivative of  $\kappa$  at  $\sigma_{vac}$ .

Color confinement is obtained by the general properties of  $\kappa$ ; it can be shown that a medium with vanishing vacuum value of the dielectric constant is color confining, i.e. net color charges would lead to infinite energy configurations [16].

Since  $\kappa$  and the  $\sigma$ -field are supposed to represent the nonperturbative structure of QCD, the gluon fields  $F_{\mu\nu}^a$  are treated as Abelian (one gluon exchange) Maxwell fields, which obey

$$\partial^\mu (\kappa F_{\mu\nu}^a) = j_\nu^a , \quad (8)$$

$$\text{with } F_{\mu\nu}^a = \partial_\mu A_\nu^a - \partial_\nu A_\mu^a , \quad (9)$$

with the color current density

$$j_\nu^a = -ig_v \bar{\Psi} \gamma_\nu \frac{\lambda^a}{2} \Psi . \quad (10)$$

All the non-Abelian features of QCD are assumed to be contained in the dielectric function  $\kappa(\sigma)$ . The other two field equations derived from the Lagrangian are then

$$(\gamma^\mu (i\partial_\mu - ig_v \frac{\lambda_a}{2} A_\mu^a) - m_0 - g_0 \sigma) \Psi = 0 \quad (11)$$

for the quarks and

$$\partial_\mu \partial^\mu \sigma + U'(\sigma) + \frac{1}{4} \kappa'(\sigma) F_{\mu\nu}^a F_a^{\mu\nu} + g_0 \rho_s = 0 \quad (12)$$

for the  $\sigma$ -field, with the scalar density  $\rho_s = \bar{\Psi} \Psi$ . The primes on  $U'$  and on  $\kappa'$  denote differentiation with respect to  $\sigma$ .

We use the following approximations: The  $\sigma$  and the  $A_\mu^a$ -field are treated as classical fields (mean field approximation). For the gluon field we choose the Coulomb gauge  $\vec{\nabla} \cdot (\kappa \vec{A}^a) = 0$  resulting in

$$\vec{\nabla}(\kappa \vec{\nabla} A_0^a) = -j_0^a, \quad (13)$$

$$-\kappa \partial_t^2 \vec{A}^a + \vec{\nabla}^2 \kappa \vec{A}^a - \vec{\nabla} \times (\kappa \vec{A}^a \times \frac{\vec{\nabla} \kappa}{\kappa}) = -\vec{j} + \kappa \vec{\nabla} \partial_t A_0^a. \quad (14)$$

In the following equation (14) is neglected as it can be shown, that currents within a flux tube do not produce a magnetic field because the displacement current is exactly cancelled by the convection current if the string radius stays nearly constant [22]. As a consequence, we determine the colorelectric field instantaneously by  $\vec{E}^a = -\vec{\nabla} A_0^a$ , which is exact in pure 1+1-dimensional electrodynamics.

The densities needed as sources for the equations (12) and (13) are provided by a transport equation derived by Elze and Heinz [23] in the semiclassical limit of an exact equation of motion for the quantum Wigner function making use of the Dirac equation (11). The corresponding equations for the phase space distribution functions for quarks ( $f$ ) and antiquarks ( $\bar{f}$ ) read [27]:

$$(p_\mu \partial^\mu - m^* (\partial_\mu m^*) \partial_p^\mu) f(x, p) = g_v p_\mu F^{\mu\nu} \partial_\nu^p f(x, p) \quad (15)$$

$$(p_\mu \partial^\mu - m^* (\partial_\mu m^*) \partial_p^\mu) \bar{f}(x, p) = -g_v p_\mu F^{\mu\nu} \partial_\nu^p \bar{f}(x, p). \quad (16)$$

We define the effective mass  $m^* = m_0 + g_0 \sigma$ , the energy  $\omega = \sqrt{\vec{p}^2 + m^{*2}}$  and a factor  $\eta = 4$  describing spin and isospin degeneracy. In terms of  $f$  and  $\bar{f}$  the scalar density is then given by

$$\rho_s = \frac{\eta}{(2\pi)^3} \int d^3 p \frac{m^*}{\omega} (f(x, p) + \bar{f}(x, p)), \quad (17)$$

and the color charge density by

$$\rho = j_0 = \frac{\eta}{(2\pi)^3} \int d^3 p (f(x, p) - \bar{f}(x, p)). \quad (18)$$

In deriving (15) and (16) the Abelian limit of the model has been used to reduce the color octet components of the currents and fields to one component denoted by  $j_0$

and  $A_\mu$ . Since all the nonabelian effects of QCD are assumed to be modeled by the  $\sigma$ -field, this assumption is justified. We therefore drop the color index here and in the following.

The equations (15) and (16) are a set of usual Vlasov equations describing the motion of charged particles in a selfconsistently generated scalar and vector field, determined by equation (12) and (13), respectively. They are solved by the so called *testparticle method* developed by Wong et al. [28], where every physical (anti-)quark is represented by an ensemble of  $N_T$  testparticles

$$f(\vec{x}, \vec{p}, t) = \sum_{i=1}^{N_T} \delta(\vec{x} - \vec{x}_i(t)) \delta(\vec{p} - \vec{p}_i(t)) , \quad (19)$$

$$\bar{f}(\vec{x}, \vec{p}, t) = \sum_{i=1}^{N_T} \delta(\vec{x} - \vec{\bar{x}}_i(t)) \delta(\vec{p} - \vec{\bar{p}}_i(t)) , \quad (20)$$

with the testparticles moving according to the Hamiltonian equations of motion:

$$\frac{d\vec{x}_i}{dt} = \frac{\vec{p}_i}{\omega_i} , \quad (21)$$

$$\frac{d\vec{p}_i}{dt} = -\frac{m^*(\vec{x}_i)}{\omega_i} \nabla_x m^*(\vec{x}_i) + g_v \vec{E}(\vec{x}_i) . \quad (22)$$

The testparticle coordinates for the antiparticle ensemble obey the same equations of motion except for  $g_v \rightarrow -g_v$ . The simulations are run in the so-called full ensemble method.

Since we work in the abelian limit of the theory, the color charge of the quarks can only be positive or negative. While this presents no problems for the mesons, color neutral baryons, which consist of three quarks, cannot be constructed in a straightforward way. We therefore work in the latter case with diquarks, which carry baryon number  $B = +2/3$  and negative color charge. Thus, in the case of mesons,  $\bar{f}$  denotes the phase-space distribution of antiquarks with  $B = -1/3$  and negative color charge, whereas in the case of baryons  $\bar{f}$  denotes the diquark distribution, again with negative color charge, but  $B = +2/3$ .

## 2.1 Static limit

Let us first examine the static limit of the transport equations. From quantum mechanics we know that the color charge density in a hadron has to vanish locally [36]

$$j_0(x) = \langle N | \hat{Q}(x) | N \rangle = \int d^3p (f(x, p) - \bar{f}(x, p)) = 0, \quad (23)$$

because the nucleon ground state  $|N\rangle$  is a color singlet and  $\hat{Q}$  an (arbitrary) color octet operator. From that we conclude that there is no colorelectric field in the groundstate, thus  $f = \bar{f}$ . As shown by Vetter et al. [26], the distribution functions have to be of a local Thomas Fermi type

$$f(x, p) = \bar{f}(x, p) = \Theta(\mu - \omega), \quad (24)$$

where we have introduced the Fermi energy  $\mu$  for the quarks. After inserting the local Thomas Fermi distributions (24) into the integral expression (17) the fermions can be integrated out to give

$$\rho_s = \bar{\Psi}\Psi = \frac{2\eta m^*}{\pi^2} \left[ \mu p_f + (m^*)^2 \log\left(\frac{m^*}{\mu + p_f}\right) \right] \Theta(\mu - m^*), \quad (25)$$

for the scalar density and

$$\rho_v = \Psi^\dagger\Psi = \frac{4\eta}{3\pi^2} p_f^3 \Theta(\mu - m^*) \quad (26)$$

for the quark density. Thus we are left with determining the soliton solution of the remaining  $\sigma$ -field equation (12). The equations (25, 26) differ from (28) in [26] by a factor of 2 because of the antiparticle contribution.

The soliton solution is constructed using a shooting method of Van Wijngaarden-Dekker-Brent [37]. We do not intend to investigate the total parameter dependence of the properties of the soliton solutions, since these have been extensively discussed elsewhere [16, 26]. Instead we restrict ourselves to adjust the model parameters in a way to reproduce the quark-number, mean mass of delta and nucleon and the rms radius of the nucleon for a typical baryon. With the parameters of this best



fit kept fixed, we use the Fermi energy  $\mu$  in order to go from the baryonic solution ( $N_Q = \int d^3r d^3p (f(x, p) + \bar{f}(x, p)) = 3$ ), resembling a quark-diquark configuration to the mesonic solution ( $N_Q = 2$ ), resembling a quark-antiquark configuration. The parameter set used to obtain these solutions is displayed in table 1, where we used  $\mu = 1.768 \text{ fm}^{-1}$  for the baryon and  $\mu = 1.9582 \text{ fm}^{-1}$  for the meson. The physical properties of these soliton solutions are shown in table 2 and 3, where the meson mass, which typically is too high in these models, can be significantly reduced by the inclusion of momentum projection methods and the colormagnetic energies [16]. The remaining properties are very well reproduced within our model approach. These groundstate solutions will be used in the following sections for dynamical applications.

### 3 The string-string interaction potential

Gluonic interactions in soliton bag models have been considered in two ways in the literature. On one hand the spin dependent one gluon exchange (OGE) interaction has been used to fit the strong coupling constant of the model to the experimentally observed  $N - \Delta$ -splitting. In these calculations a gluonic propagator developed by Bickeboeller et al. [34] is used, resulting in a value for  $\alpha_s \approx 2$  [32, 38, 39, 40, 41]. Although it is in principle possible to determine the OGE matrix elements for dynamical systems without any special spatial symmetry, the calculation of the propagators is very involved and has therefore not yet been performed. On the other hand there have been flux tube solutions constructed with an infinite (cylindrical) geometry assuming a large mass for the quark-antiquark pair at the endcaps of the tube (Born-Oppenheimer approximation) and an instantaneous colorelectric field between them [34, 42]. Within these approximations the most important property of the tube, the string tension  $\tau \approx 1 \text{ GeV}/\text{fm}$ , has been fitted, where again values of the strong coupling constant  $\alpha_s \approx 2$  have been obtained.

We proceed differently here and calculate first the response of the colorelectric field to an adiabatic separation of the quark-antiquark pair of the meson ground-

state, i. e. the quark and antiquark move apart with a given constant velocity which is taken to be  $v_q = -v_{\bar{q}} = 0.1c$  in order to guarantee adiabaticity in our calculations. The quark degrees of freedom are taken as frozen, so that the spatial shape of the quark distributions is not changed during this process. The corresponding field equations (12) and (13) are solved selfconsistently throughout the time evolution via a staggered leapfrog algorithm for the complete (3-dimensional)  $\sigma$ -field [26] combined with a (2-dimensional) finite element method for the colorelectric field [43], exploiting the cylindrical symmetry of the system. In this way we dynamically generate a color dielectric flux tube with a length of  $8 fm$  and a width of  $\approx 1 fm$  as described in [27] and fix the strong coupling constant  $\alpha_s$  to a string constant of  $\tau = 1 GeV/fm$ , obtaining  $\alpha_s = 1.92$ , in agreement with the earlier estimates discussed above.

Similarly we can construct a two flux tube configuration with either parallel or antiparallel colorelectric fields as schematically depicted in figure 1. Starting with this configuration we let the quarks inside the different tubes move with a constant and fixed fusion velocity  $v_f = 0.1 c$  towards each other keeping their spatial shape fixed throughout the fusion process. We have checked that at this low fusion velocity the  $\sigma$ -field follows the quark motion without retardation. We finally extract an interaction potential  $V_{ad}$  for the two strings via [44]

$$V_{ad}(\rho) = E_\sigma(\rho) + E_{gl}(\rho) - E_\sigma(\infty) - E_{gl}(\infty) , \quad (27)$$

with

$$E_\sigma = \int d^3r \left( \frac{1}{2}(\nabla\sigma)^2 + U(\sigma) + g_0\sigma\rho_s(\sigma) \right) , \quad (28)$$

$$E_{gl} = \frac{1}{2} \int d^3r \kappa(\sigma) \vec{E}^2 . \quad (29)$$

The interaction potential is taken to be the difference in the field energies compared to infinitely separated strings as a function of the transverse distance  $\rho_t$  of the tubes.

Due to the loss of the cylindrical symmetry in this scenario, we adopt the following prescription for determining the colorelectric field: We take the axis connecting the quark and antiquark of one of the flux tubes as the symmetry axis. The colorelectric

field is then calculated taking only the color charges within this tube into account, resulting in an 'undisturbed' field configuration  $\vec{E}_u$ , as for instance shown in one of the tubes in the upper picture of figure 2. The total colorelectric field is assumed to be given by

$$\vec{E}(x, y, z) = \vec{E}_u(x - \rho_t, y, z) \pm \vec{E}_u(x + \rho_t, y, z) , \quad (30)$$

where the plus sign is valid for parallel tubes and the minus sign for antiparallel ones. The index  $u$  denotes the 'undisturbed' field configuration and  $\rho_t$  stands for the (transverse) distance of the symmetry axis of the individual tube to the x-axis. We consider this coherent addition of the undisturbed colorelectric fields to be a strong assumption, since we neglect the direct interaction of the individual quark with both quarks of the neighboring flux tube. However, in the limit  $\rho_t \rightarrow 0$ , the cylindrical symmetry is restored and our prescription is valid again. Furthermore, the equation for the  $\sigma$ -field is solved with the full 3+1-dimensional technique developed by Vetter et al. [26]. A complete 3-dimensional finite-element treatment of both, the Poisson equation (13) and the  $\sigma$ -field equation (12), is in preparation [45].

The result for the *parallel* configuration is shown in figure 3, where one can see that there is no long range interaction in this model due to confinement [42] for distances larger than 1  $fm$ . But as soon as the tubes get in touch with each other at distances less than 1  $fm$ , the confinement wall between them breaks down and we gain surface energy from the  $\sigma$ -field (3). The short range behaviour is strongly repulsive, which is clarified in figure 2, where the field configurations are shown for the  $\sigma$ -field (left side) and the colorelectric field (right side) throughout the adiabatic fusion: when the charges start to overlap, the coherent addition of the colorelectric field leads to a doubling of the  $\vec{E}$ -field and thus to 4 times the colorelectric energy in the complete overlap configuration. This rise in energy results in the strong short range repulsion of the parallel strings. The adiabatic string-string potential is qualitatively very similar to the nucleon-nucleon potential in the same model obtained by Koepf et al. [44], which has been calculated as the energy difference of a deformed six-quark bag and two noninteracting separated nucleons. We even get quantitative

agreement with those calculations if we scale the potential with the length  $L$  of the flux tube, which is shown in figures 3 and 4.

For the *antiparallel* configuration (figure 4) again there is no long range interaction. However, as soon as the confinement wall of the flux tubes starts to break down, we get an attraction coming from the decrease in energy of the  $\sigma$ -field. An even larger attraction results from the colorelectric field, since the two opposite color charges at the end of the tubes neutralize each other, so that the color field vanishes at very low transverse distances and the flux tube collapses.

Our model then supports the independent string picture, which is, for instance, phenomenologically used in the Lund code [6]. That means that the parallel strings repel each other, building an ensemble of single individual strings. Antiparallel strings, on the other hand, do prefer to fuse and neutralize the color charges at the endcaps, leading to a collapse of the flux tube.

## 4 Flux tube breaking

In this section we show how a flux tube of the Friedberg-Lee model breaks up due to quark-antiquark pair production. One usually describes such processes with the Schwinger formula [20], which gives a constant pair production rate of electron-positron pairs in QED, depending only on the absolute value of the electric field. However, this formula cannot be naively transferred to the QCD case of  $q\bar{q}$ -production in a flux tube for very different reasons.

First of all, the back reaction of the produced pairs on the external field has to be considered [46], since this screening of the field is finally responsible for the breakup of the strings. Furthermore one must consider the modifications of the pair production rate due to transverse and longitudinal confinement [5, 20, 21, 47, 48, 49]. Besides many other issues, these authors have shown in various bag models, that the production rate is strongly suppressed due to the reasons mentioned above.

However, a detailed analysis of the time dependent pair production process within

the Friedberg-Lee model has not yet been performed. Therefore we have to rely on different phenomenological arguments, providing us with a simple guideline to the space-time evolution of a fragmenting string.

The earliest and most successful model of string fragmentation is the Lund-model [50]. Within this model one assumes the quarks to be massless and therefore moving with the speed of light. Even the original  $Q\bar{Q}$ -pair, generating the string, is supposed to travel on the lightcone. Within these assumptions it is sufficient to describe the fragmentation process by a 1+1-dimensional space-time geometry, for it is causally impossible that the produced  $q\bar{q}$ -pairs propagate towards the endcaps (the  $Q\bar{Q}$ -pair).

Four of the most simple string fragmentation diagrams emerging from this model are shown in the figures 5 a) - 5 d). The figures show the propagation of the original  $Q\bar{Q}$ -pair and the consecutively produced  $q\bar{q}$ -pairs under the influence of a constant and therefore confining colorelectric field. In figure 5 a) we show the breakup of the string due to the production of one pair in the center of the string and the symmetric and equal-time production of two pairs in figure 5 b). In both cases excited meson states emerge, travelling with the rapidity of the original quarks, whereas in the second case an excited 'Yo-Yo'-state with vanishing velocity is formed in addition. In figure 5 c) and 5 d) the breakup of a string via equal- and non-equal-time production of three  $q\bar{q}$ -pairs is presented. In the first case the final excited 'Yo-Yo'-modes again have a vanishing total momentum whereas in the latter case their total momentum is nonvanishing, with its value depending on the difference in production time.

There are two physical properties of the final mesons that are fixed by the model parameters [6, 50]: the mass of the final fragments can be fixed by choosing the space-time breakup points appropriately, according to

$$t^2 - x^2 = 2m^2/\tau^2, \quad (31)$$

where  $m$  is the mass of the final meson and  $\tau$  the string-constant. The second property to be fixed is the rapidity distribution of the final fragments, that can be chosen

through the so called *fragmentation function* [6, 50]. Within the range of only a few parameters, that are fitted to  $e^+e^-$ -data, a very reasonable description of particle spectra for hadron-hadron and heavy-ion collisions can be obtained. Motivated by these results we present in the following a fully dynamical space-time description of the fragmentation processes shown in figure 5 within our model approach.

## 4.1 The Transport Dynamical Model

As a prerequisite we assume that the original  $Q\bar{Q}$ -pair travels with the speed of light along the  $\pm z$ -axis, irrespective of the interior dynamics, which is generated by solving selfconsistently the transport equations (15) and (16) together with the mean-field equations for the  $\sigma$ -field (12) and the colorelectric field (13) with the numerical techniques described in the previous section. The source densities entering the field equations are determined via the integral relations (17) and (18). The produced  $q\bar{q}$ -pairs are inserted into the dynamically evolving flux-tube by assuming their groundstate spatial shape that has been determined in the previous section and with a vanishing total momentum [22]. Each quark of the produced  $q\bar{q}$ -pairs is represented by a testparticle ensemble with  $N_T = 50000$ .

In figure 6 we show the color charge density  $\rho = j_0$ , the energy density of the colorelectric field  $\epsilon = \frac{1}{2}\kappa\mathbf{E}^2$  and the scalar  $\sigma$ -field along the longitudinal and transverse axis. In the upper row, at  $t = 1.8 fm/c$ , the quarks have a distance of  $3.6 fm$  and the colorelectric field between them together with the confining cavity of the  $\sigma$ -field builds up. At  $t = 2 fm/c$  the  $q\bar{q}$ -pair is inserted and instantaneously torn apart by the force of the colorelectric field. In the second row, at  $t = 2.6 fm/c$ , we see that the separating  $q\bar{q}$ -pair causes a screening of the colorelectric field in the region between them, where the energy density of the color field already vanishes. Consequently, but with a little delay in time, the  $\sigma$ -field is beginning to snap off in the screening region. In the lower two rows, at  $t = 3.4 fm/c$  and  $t = 7.0 fm/c$  the free propagation of the final string fragments can be seen, where we observe some

slight late oscillations of the  $\sigma$ -field due to its inert behaviour caused by the large glueball mass. Overall, the observed time development corresponds to the expected space-time behaviour shown in figure 5 a). In the lower row of figure 6 we recognize a small dispersion of the  $q$  and  $\bar{q}$  distributions, which is caused by the selfinteraction of the quarks, leading to a screening of the charges: a charge fragment at the end of one of the two substrings feels a smaller colorelectric force due to its interaction with the charge fragments in front of it.

As a further example we show in figure 7 the space-time evolution of the string fragmentation via equal time production of three  $q\bar{q}$ -pairs, in analogy to figure 5 c). In the upper row at  $t = 2.8 fm/c$ , the string is already extended to a length of  $5.6 fm$ ; the constant colorelectric field along the string is reflected in the constant field energy between the charges. At  $t = 3.0 fm/c$  the three  $q\bar{q}$ -pairs are inserted at  $z = 0 fm$  and  $z = \pm 2.0 fm$  with a vanishing relative velocity.

In the second row at  $t = 3.6 fm/c$  we once again see the screening effect from the motion of the quarks inside the flux-tube and consecutively the beginning of the snapping off of the  $\sigma$ -field. In the following we observe, as in the previous example, the formation of the outer two meson pairs propagating on the lightcone. In the inner region of the flux-tube, the respective quark pairs penetrate each other, having already acquired a small dispersion. At the time  $t = 4.2 fm/c$ , the colorelectric field is almost completely screened. This abrupt change of the colorelectric field, being also a source of the  $\sigma$ -field (see eq. (12)), leaves the  $\sigma$ -field highly excited. Therefore the  $\sigma$ -field snaps off and starts to oscillate around the nonperturbative vacuum value  $\sigma_{vac}$ . These oscillations can be followed in the last two timesteps of figure 7, where  $\sigma \approx 0$  in the center of the string at  $z = 0 fm$  and  $\sigma \approx \sigma_{vac}$  around. Comparison with the leftmost column in figure 7 shows that the  $\sigma$ -field, which is supposed to localize the quarks, cannot prevent a further dispersion of the color charges and the latter neutralize and dissolve along the  $z$ -axis to a length of about  $8 fm$  at  $t = 8.4 fm/c$ . As a consequence the scalar density of the quarks is reduced by almost an order of magnitude.

In this case the  $\sigma$ -field undergoes a complete phase transition to the nonperturbative vacuum, since this is energetically more favorable, which is clarified in figure 8. There it can be seen, that the global minimum of the effective selfinteraction potential

$$U_{eff}(\sigma) = U(\sigma) + g_0\sigma\rho_s \quad (32)$$

is at  $\sigma_{vac}$ , if the scalar density drops below 1/3 of the groundstate density. After returning to  $\sigma_{vac}$ , the field undergoes damped oscillations, irrespective of the remaining  $q\bar{q}$ -fragments.

## 4.2 The Molecular Dynamical Model

As already mentioned, in the present numerical realization of our model each testparticle of the respective ensembles interacts not only with the testparticles of the other quarks, but also with the testparticles of the same quark. This selfinteraction, which leads to the dispersion of the quark distributions, becomes dominant in the limit of only a few interacting physical particles; in the extreme case, a single color charge distribution with an almost vanishing mass would immediately dissolve due to the selfinteraction. Unlike in other models, like e. g. the Walecka-model, which also contains an attractive scalar field and a repulsive vector field and which has been treated successfully [24], in the present case the attractive  $\sigma$ -field acts only in transverse direction on the produced quarks. Its longitudinal effect is completely suppressed by the colorelectric field. Thus we are forced to formulate a new dynamical approach, that conserves the identity of the different quarks and antiquarks and is free of the selfinteraction problem.

A possible way to overcome the problems mentioned above is to treat the quarks in a molecular dynamical framework. In this approach each physical particle (quark or antiquark) is simulated by just one testparticle and not by an ensemble of testparticles ( $N_T = N_{phys}$ ) in the equations (19) and (20). Due to the fact that point-like particles cause short range divergences in the field equations, a specific spherically symmetric



distribution is assigned to each individual testparticle. In our case we choose this distribution to be the meson groundstate distribution, as we have calculated in the previous section. This provides us with the scalar density  $\rho_s$  and the charge density  $\rho$  of each individual (anti-)quark. Although violating Lorentz covariance, we keep the spatial shape fixed throughout the time evolution, as a first approach to the reaction dynamics. A testparticle then describes the motion of the center of its distribution according to the Hamiltonian equation of motion (21). The initial momentum of the produced (anti-)quarks is chosen to vanish [22], and propagated according to the equation (22) afterwards. The total scalar density and charge density entering the field equations (12) and (13) is given by the sum over all (anti-)quarks. The field equations, on the other hand, are simulated by the same techniques as in the full transport dynamical model.

In the following we show how we obtain a space-time description of the diagram of figure 5 d), thus presenting a fully dynamical description of the disintegration of a flux-tube into a multiple (excited) meson state within the Friedberg-Lee model.

The corresponding space-time evolution of this process can be followed in figures 9 and 10, where once again the color charge density  $\rho$ , the energy density of the colorelectric field  $\epsilon$  and the  $\sigma$ -field is presented at eight different time steps, which are chosen such, that all relevant steps of the diagram 5 d) can be followed. We start our presentation at  $t = 2.7 fm/c$ , shortly after the first  $q\bar{q}$ -pair has been inserted in the coordinate center. We see that the quarks of this first  $q\bar{q}$ -pair already propagate along their respective directions and observe a prompt screening of the colorelectric field in the center, whereas the more inert  $\sigma$ -field has not yet changed significantly. In the second row of figure 9, at  $t = 3.2 fm/c$ , the remaining two  $q\bar{q}$ -pairs have just been inserted at  $z = \pm 2 fm$  at  $t = 3.0 fm/c$  and are moving under the influence of the colorelectric field. We see how the screening proceeds not only at the coordinate center, but also between the other fragments. The confining  $\sigma$ -field still shows no reaction to the interior dynamics. In the third row we clearly see how the two lightcone fragments have been formed as well as the two excited 'Yo-Yo'-modes

in between after  $5.4 fm/c$ . The motion of the latter at this particular timestep is such that the distributions almost completely sit on top of each other, so that the colorelectric field vanishes.

We additionally clearly see how the confining  $\sigma$ -field starts to form around the final fragments. This process is completed after  $7.2 fm/c$  as we find in the lower row of figure 9, where the  $\sigma$ -field again undergoes slightly damped oscillations in the regions of the nonperturbative vacuum. Due to the different production times of the inner  $q\bar{q}$ -pairs, the respective pairs of the final fragments have a nonvanishing total momentum when forming an excited meson and thus start to propagate along the z-axis as can also be seen in this figure.

The late time evolution of this reaction is shown in the figure 10 at the time steps  $t = 7.8, 8.6, 10.6, 12.2 fm/c$ ; note the rescaled z-axis for presentational purposes. During this late time development we find a more or less complete correspondence of the dynamical behaviour of our model with the 1+1-dimensional Lund-diagram 5 d). We see the propagation of the final fragments as well as the remaining 'Yo-Yo'-modes of the inner two excited mesons. The latter are obviously undamped as expected from the simple diagrammatic representation.

## 5 Discussion, Summary and Outlook

We have presented two novel features of flux tubes in the Friedberg-Lee model. First we have extracted a string-string interaction potential by an adiabatic fusion of two parallel or antiparallel strings. The potential is obtained by comparing the colorelectric and the  $\sigma$ -field energies of the fused configuration to the (infinitely) separated configuration. For the parallel strings it shows a qualitative similarity to the nucleon-nucleon-potential of Koepf et al. [44], which has been calculated in a similar way as the energy difference of a deformed six-quark bag and two noninteracting separated nucleons. Therefore it seems to be a general feature of the Friedberg-Lee model, that the interaction of two color neutral objects (nucleons, parallel strings) can be

described in the following way:

Due to confinement in this model there is no long range interaction (over distances typically of the order of  $1 fm$  and more). In the intermediate range, when the confinement wall starts to break down, we have a balance of gaining surface energy from the  $\sigma$ -field and increasing the total energy from the coherent addition of the colorelectric field. In the short range region the potential is strongly repulsive due to the unscreened quark color charges at the endcaps in the case of parallel strings, and in the NN-interaction due to the unscreened (aligned) color spins of the quarks. In the case of antiparallel strings, however, a strong attraction is found leading to a neutralization of the color charges and the collapse of the flux tube.

Secondly we have shown how the flux-tube breaking proceeds in the Friedberg-Lee model. Since no estimates of the pair production rate in this model have been performed so far, we give a space-time description of some of the simplest Lund-type diagrams. We have shown the full transport dynamical behaviour of the quark and antiquark distributions for a string fragmenting via the production of one  $q\bar{q}$ -pair and three  $q\bar{q}$ -pairs at an equal time. In the first case the space-time behaviour of two meson pairs propagating on the light-cone can be reproduced by our model. In the latter case of three produced  $q\bar{q}$ -pairs, the outer meson pairs are also formed, but in the center of the fragmenting string, where the two parallel 'Yo-Yo'-modes are supposed to build up, we observe a different behaviour:

When the respective quark distributions start to penetrate and neutralize, a small dispersion of these is already observed. At this time the colorelectric field is completely screened in the center of the string. This sudden change of the source of the flux-tube leaves the  $\sigma$ -field highly excited and thus it starts to oscillate around the nonperturbative vacuum value. The  $\sigma$ -field is not able to prevent the further dispersion of the quark distributions, which neutralize and dissolve along the string-axis. With the scalar density being significantly reduced in this case, the  $\sigma$ -field undergoes a complete phase transition to the nonperturbative vacuum.

Therefore we have to face the following problems within this realization of the

dynamical model:

First of all the large value of the strong coupling constant  $\alpha_s = 1.92$ , being responsible for the large energy density of the colorelectric field, leads to a very deep flux-tube, with values of the  $\sigma$ -field up to  $-\sigma_{vac}$ , whereas the perturbative region is thought to be around  $\sigma \approx 0$ . Therefore the  $\sigma$ -field is highly excited when the quark charges are screened, causing large amplitude oscillations that are only slowly damped. In order to avoid these oscillations and provide a faster damping, one might think of an additional coupling of the  $\sigma$ -field to its chiral partner, the pion-field, in the chirally symmetric O(4)-version of the model [51, 52, 53]. By this extension, the oscillations of the  $\sigma$ -field can be used to excite low mass pion-modes, that disperse the energy of the  $\sigma$ -field effectively.

Additionally one could determine a new parameter set of the model. A lowering of the bag-constant, for instance, would facilitate the string-formation, as well as the fragmentation. However, the present value of  $B = 56 \text{ MeV}/fm^3$  is already in the lower region of the ones that are generally used. A larger value of the scalar coupling constant  $g_0$  would facilitate the formation of bags and thus the localization of the quarks in a perturbative region.

The second problem is the dispersion of the quark distributions, which is caused by their selfinteraction. This dispersion is an artefact of our numerical method, for we deal with only a few quarks that are treated as classical charge distributions and interacting strongly via a classical confining potential. In this case the selfinteraction of the color charges becomes dominant and generates a screening of the charges, which finally is responsible for the dispersion of these.

We have shown a possible way to overcome these problems by treating the quarks and antiquarks as point particles with an appropriately chosen charge distribution as commonly used in molecular dynamical simulations. We have shown within a first and simple approach, where we keep the spatial shapes of these distributions fixed, how the Lund-type dynamics of the string-fragmentation can be reproduced for even more complex Lund-diagrams. An improvement of the molecular dynamical approach

can be achieved by implementing a time-dependent radius or dipole-moment of the quark distribution. These multipole moments could account for Lorentz contraction, polarization effects of the distributions or monopole oscillations.

Summarizing we can say that our model provides us with a useful tool to describe the full dynamical evolution of string formation and decay via multiple quark-antiquark production. The aim for future investigations should be to apply our model to more realistic scenarios, like multiple string production and decay in relativistic heavy-ion collisions, for describing the formation of hadrons out of an expanding and cooling quark-gluon plasma.

## References

- [1] R. Anishetti, P. Koehler and L. McLerran, Phys. Rev. **D22** (1980) 2793
- [2] J. D. Bjorken, Phys. Rev. **D27** (1983) 140
- [3] T. S. Biro, B. H. Nielsen and J. Knoll, Nucl. Phys. **B245** (1984) 449
- [4] A. Bialas and W. Czyz, *Quark-Gluon Plasma*, ed. R. C. Hwa (Singapore, World Scientific) (1990) p. 271
- [5] K.Sailer, Th. Schnfeld, Zs. Schram, A. Schfer and W. Greiner, Jour. Phys **G** (1991), Nucl. Part. Phys. **17** 1005
- [6] B. Andersson, G. Gustafson and B. Nielsson-Almquist, Nucl. Phys. **B281** (1987) 289
- [7] K. Werner, Z. Phys. **C42** (1989) 85
- [8] H. Sorge, H. Stcker and W. Greiner, Nucl. Phys. **A498** (1989) 567c
- [9] X.-N. Wang and M. Gyulassy, Phys. Rev. **D44** (1991) 3501
- [10] K. Geiger and B. Mller, Nucl. Phys. **B369** (1992) 600

- [11] K. Geiger, Phys. Rev. **D51** (1995) 3669
- [12] J. Ellis and K. Geiger, Phys. Rev. **D52** (1995) 1500
- [13] T. DeGrand, R. L. Jaffe, K. Johnson and J. Kiskis, Phys. Rev. **D 12** (1975), 2060
- [14] R. Alkofer, H. Reinhardt and H. Weigel, Lanl hep-ph/9501213
- [15] C. V. Christov, A. Blotz, H. C. Kien, P. Pobylitsa, T. Watabe, T. Meissner, E. Ruiz Arriola and K. Goeke, Prog. Part. Nucl. Phys. **37** (1996) in print
- [16] L. Wilets, *Nontopological Solitons*, Lecture Notes in Physics, Vol. 24 (World Scientific, Singapore 1989) and references therein
- [17] R. Friedberg and T.D. Lee, Phys. Rev. **D15**(1977) 1694 and **D16** (1977) 1096
- [18] H. B. Nielsen and A. Patkos, Nucl. Phys. **B195** (1982) 137
- [19] M. C. Birse, Prog. Part. Nucl. Phys. **A448** (1990) 557
- [20] H. P. Pavel and P. M. Brink, Z. Phys. **C51** (1991) 119
- [21] I. D. Flintoft and M. C. Birse, J. Phys. **G 19** (1993) 389
- [22] L. Wilets and R. D. Puff, Phys. Rev **C 51** (1995) 339
- [23] H.Th. Elze and U. Heinz, Phys. Rep. 183 (1989) 81
- [24] B. Blttel, V. Koch and U. Mosel, Rep. Prog. Phys. **56** (1993) 1
- [25] U. Kalmbach, T. Vetter, T. S. Biró and U. Mosel, Nucl. Phys. **A563** (1993) 584
- [26] T. Vetter, T. S. Biró and U. Mosel, Nucl. Phys. **A581** (1995) 598
- [27] S. Loh, T. S. Biro, U. Mosel and M. H. Thoma, Phys. Lett. **B387** (1996) 685
- [28] C. Y. Wong, Phys. Rev. **C 45** (1982) 1460

- [29] R. Friedberg and T.D. Lee, Phys. Rev. **D18** (1978) 2623
- [30] R. Goldflam and L. Wilets, Phys. Rev. **D25** (1982) 1951
- [31] L. Wilets, M.C. Birse, G. Lbeck and E.M. Henley, Nucl. Phys. **A434** (1985) 129
- [32] M. Bickebller, M.C. Birse and L. Wilets, Z. Phys. **A326** (1988) 89
- [33] T. D. Lee, Phys. Rev. **D19** (1979) 1802
- [34] M. Bickebller, M.C. Birse, H. Marschall and L. Wilets, Phys. Rev. **D31** (1985) 2892
- [35] R. Goldflam and L. Wilets, Comments Nucl. Part. Phys. **12** 191, (1984)
- [36] U. Mosel, *Fields, Symmetries and Quarks*, McGraw-Hill (1989)
- [37] W. H. Press, S. A. Teukolsky, W. T. Vetterling, and B. P. Flannery, *Numerical Recipes*, Second Edition, Cambridge University Press, Cambridge, 1992
- [38] Q. Haider and L. C. Liu, J. Phys. **G12** (1986) L75
- [39] L. R. Dodd and A. G. Williams, Phys. Lett. **B210** (1988) 10
- [40] N. Aoki and H. Hyuga, Nucl. Phys. **A505** (1989) 525
- [41] S. Sahu, Nucl. Phys. **A554** (1993) 721
- [42] M. Grabiak and M. Gyulassy, J. Phys. **G 17** (1991), 583
- [43] W. F. Mitchell, *Unified Multilevel Adaptive Finite Element Methods for Elliptic Problems*, PhD Thesis University of Illinois, (1988)
- [44] W. Koepf, L. Wilets, S. Pepin and Fl. Stancu, Phys. Rev. **D50** (1994) 614
- [45] C. Traxler, *An Algorithm for Adaptive Mesh Refinement in n Dimensions*, Computing (in print)

- [46] N. K. Glendenning, T. Matsui, Phys. Rev. **D28** (1983) 2890
- [47] K. Sailer, Th. Schnfeld, A. Schfer, B. Mller, W. Greiner, Phys. Lett. **B240** (1990) 381
- [48] K. Sailer, Z. Hornyak, A. Schfer, W. Greiner, Phys. Lett. **B287** (1992) 349
- [49] C. Wong, R. Wang, J. Wu, Phys. Rev. **D51** (1995) 3940
- [50] B. Andersson, G. Gustafsson, G. Ingelmann, T. Sjstrand, Phys. Rep. **97** (1983) 33
- [51] H. Kitagawa, Nucl. Phys. **A487** (1988) 544
- [52] A. Drago, K. Bruer, A. Fessler, J. Phys. **G15** (1989) L7
- [53] T. Neuber, M. Fiolhais, K. Goeke, J. N. Urbano, Nucl. Phys. **A560** (1993) 909



Figure 1: Parallel and antiparallel flux tube configurations drawn schematically.

Figure 2: The cavity of the  $\sigma$ -field and the colorelectric field throughout the adiabatic fusion process of parallel flux-tubes. The transverse distance of the tubes is (from top to bottom):  $\rho = 1.75, 1.25, 0.75, 0.25 fm$ . The equidistant contour lines start at  $-0.125 fm^{-1}$  to  $0.25 fm^{-1}$  (in the lower row from  $-0.175 fm^{-1}$  to  $0.25 fm^{-1}$ ).

Figure 3: Adiabatic string-string potential for the parallel configuration. The solid line shows the sum of the contributions from the  $\sigma$ - and the colorelectric field.

Figure 4: Adiabatic string-string potential for the antiparallel configuration. The solid line shows the sum of the contributions from the  $\sigma$ - and the colorelectric field.

Figure 5: Space-time representation of some of the simplest Lund stringfragmentation graphs.

Figure 6: The figure shows the time evolution of the color charge density  $\rho$ , the energy density of the colorelectric field  $\epsilon$  and the  $\sigma$ -field for the breakup of the string via the production of one  $q\bar{q}$ -pair. For calculating the motion of the quarks the full transport dynamics have been used. The equidistant contour lines run from  $-0.5 fm^{-3}$  to  $0.5 fm^{-3}$  for  $\rho$ , from  $0.0 fm^{-4}$  to  $4.0 fm^{-4}$  for  $\epsilon$  and from  $-0.15 fm^{-1}$  to  $0.25 fm^{-1}$  for  $\sigma$ . The respective charges of the generating  $Q\bar{Q}$ -pair are indicated by a + or - sign.

Figure 7: The figure shows the time evolution of the color charge density, the energy density of the colorelectric field and the  $\sigma$ -field for the breakup of the string via the production of three  $q\bar{q}$ -pairs. For calculating the motion of the quarks the full transport dynamics has been used. The equidistant contour lines run from  $-0.5 \text{ fm}^{-3}$  to  $0.5 \text{ fm}^{-3}$  for  $\rho$ , from  $0.0 \text{ fm}^{-4}$  to  $3.0 \text{ fm}^{-4}$  for  $\epsilon$  and from  $-0.125 \text{ fm}^{-1}$  to  $0.25 \text{ fm}^{-1}$  for  $\sigma$ . The respective charges of the generating  $Q\bar{Q}$ -pair are indicated by a + or - sign.

Figure 8: The effective selfinteraction potential for different values of the scalar density, starting from the solid line to the dotted line:  $0.110 \text{ fm}^{-3}$ ,  $0.072 \text{ fm}^{-3}$ ,  $0.050 \text{ fm}^{-3}$ ,  $0.043 \text{ fm}^{-3}$ ,  $0.036 \text{ fm}^{-3}$ ,  $0.021 \text{ fm}^{-3}$ ,  $0.000 \text{ fm}^{-3}$ .

Figure 9: The figure shows the early time evolution of the color charge density, the energy density of the colorelectric field and the  $\sigma$ -field for the breakup of the string via the production of three  $q\bar{q}$ -pairs at different time steps  $t = 2.7, 3.2, 5.4, 7.2 \text{ fm}/c$ . For calculating the motion of the quarks the molecular dynamical approach has been used. The equidistant contour lines run from  $-0.35 \text{ fm}^{-3}$  to  $0.35 \text{ fm}^{-3}$  for  $\rho$ , from  $0.0 \text{ fm}^{-4}$  to  $3.0 \text{ fm}^{-4}$  for  $\epsilon$  and from  $-0.15 \text{ fm}^{-1}$  to  $0.25 \text{ fm}^{-1}$  for  $\sigma$ .

Figure 10: The figure shows the late time evolution of the color charge density, the energy density of the colorelectric field and the  $\sigma$ -field for the breakup of the string via the production of three  $q\bar{q}$ -pairs at different time steps  $t = 7.8, 8.6, 10.6, 12.2 \text{ fm}/c$ . For calculating the motion of the quarks the molecular dynamical approach has been used. The equidistant contour lines run from  $-0.35 \text{ fm}^{-3}$  to  $0.35 \text{ fm}^{-3}$  for  $\rho$ , from  $0.0 \text{ fm}^{-4}$  to  $3.0 \text{ fm}^{-4}$  for  $\epsilon$  and from  $-0.15 \text{ fm}^{-1}$  to  $0.25 \text{ fm}^{-1}$  for  $\sigma$ .

parameter set	
$a$ [ $fm^{-2}$ ]	0.0
$b$ [ $fm^{-1}$ ]	-419.3
$c$ [1]	4973.0
$B$ [ $fm^{-4}$ ]	0.283
$g_0$ [1]	8.0
$m_0$ [ $fm^{-1}$ ]	0.025
$\mu$ [ $fm^{-1}$ ]	1.768 / 1.9582
$\eta$	4
$\sigma_{vac}$ [ $fm^{-1}$ ]	0.253
glueball mass [ $GeV$ ]	1.045

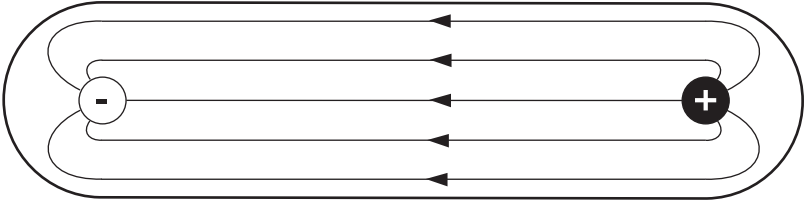
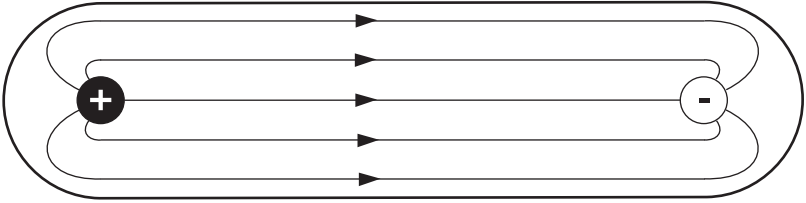
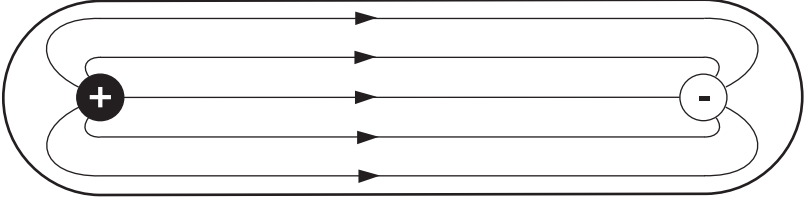
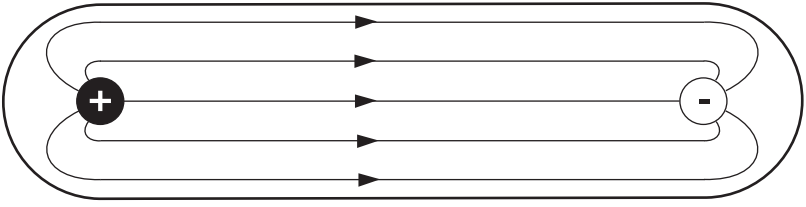
Table 1: The table shows the parameters used to construct a mesonic and a baryonic soliton solution of the sigma field equation. The first value of  $\mu$  is used for the baryonic solution, the second one for the mesonic.

Parameter set	meson	Experimental Data
$E$ [MeV]	798	465
$RMS$ [fm]	0.653	0.66

Table 2: The table shows the results of the fits for the meson compared to the experimental data. The experimental data are the mean values of the pion and the rho-meson (taken from [16]).

Parameter set	baryon	Experimental Data
$E$ [MeV]	1099	1087
$RMS$ [fm]	0.693	0.83

Table 3: The table shows the results of the fit for the baryon compared to the experimental data. The experimental data are taken from [16].



p

p

